Fabrication of Truncated Rhombic Dodecahedral Cu 2 O Nanocages and Nanoframes by Particle Aggregation and Acidic Etching

ARTICLE *in* JOURNAL OF THE AMERICAN CHEMICAL SOCIETY · SEPTEMBER 2008

Impact Factor: 12.11 · DOI: 10.1021/ja804625s · Source: PubMed

2 AUTHORS, INCLUDING:

Chun-Hong Kuo
Academia Sinica
25 PUBLICATIONS **2,150** CITATIONS

SEE PROFILE

J|A|C|S
ARTICLES

Published on Web 08/30/2008

Fabrication of Truncated Rhombic Dodecahedral Cu_2O Nanocages and Nanoframes by Particle Aggregation and Acidic Etching

Chun-Hong Kuo and Michael H. Huang*

Department of Chemistry, National Tsing Hua University, Hsinchu 30013, Taiwan

Received June 17, 2008; E-mail: hyhuang@mx.nthu.edu.tw

Abstract: We report a simple approach for the fabrication of cuprous oxide (Cu_2O) nanocages and nanoframes possessing an unusual truncated rhombic dodecahedral structure. An aqueous solution containing $CuCl_2$, sodium dodecyl sulfate (SDS) surfactant, $NH_2OH \cdot HCl$ reductant, HCl, and NaOH was prepared, with the reagents introduced in the order listed. Rapid seed-particle aggregation and surface reconstruction of the intermediate structure resulted in the growth of type-I nanoframes, which have only {110} skeleton faces and empty {100} faces, 45 min after mixing the reagents. Continued crystal growth for additional 75 min produced nanocages with filled {100} faces. The nanocages have diameters of 350−400 nm, and their walls are thicker than those of the nanoframes. Selective acidic etching over the {110} faces of the nanocages by HCl via the addition of ethanol followed by sonication of the solution led to the formation of type-II nanoframes, which have elliptical pores on the {110} faces. The morphologies of these nanoframes were carefully examined by electron microscopy. Without addition of ethanol, random etching of the nanocages can occur at a slow rate. Octahedral gold nanocrystals and high-aspect-ratio gold nanorods were successfully encapsulated in the interiors of these Cu_2O nanocages by adding the gold nanostructures into the reaction solution. The formation process for such core−cage composite structures was studied. These composite materials should display interesting properties and functions.

Introduction

Cuprous oxide (Cu_2O) is a p-type semiconductor with a direct band gap of 2.17 eV. Cu_2O nanostructures have been demonstrated to possess properties useful for applications in gas sensing,[1,2] CO oxidation,[3] photocatalysis,[4] photoactivated splitting of water,[5] and organic synthesis.[6] In the past few years, numerous Cu_2O nanostructures, including nanoplates,[7] nanocubes,[8,9] octahedra,[10,11] spherical particles,[12] nanocages,[13−17] and nanowires,[18−20] have been synthesized. Among these morphologies, nanocages may exhibit better catalytic activities because of their higher surface areas. So far, Cu_2O nanocages with octahedral,[13] cubic,[14,16] spherical,[15] and multishelled spherical[17] shapes have been prepared. However, syntheses of Cu_2O nanocages and nanoframes with more exotic morphologies have not been reported. Generally, there are two major approaches for preparing hollow nanostructures. The most common method involves the use of templates that serve as cores for the subsequent growth of the shells.[21−23] The cores need to be removed by dissolution, etching, or thermal treatment. Templateless synthesis by self-construction, which is based on the ability of spherical nanocrystallites to stabilize certain crystallographic planes as they undergo two-dimensional (2D) and then 3D aggregation, represents another mechanism for fabricating hollow nanostructures.[14,15,24] Despite these two useful strategies, the synthesis of oxide nanocages having well-defined geometries and controllably or selectively etched faces through the use of a simple solution system has rarely been demonstrated.

(1) Zhang, J.; Liu, J.; Peng, Q.; Wang, X.; Li, Y. *Chem. Mater.* **2006**, *18*, 867.
(2) Zhang, H.; Zhu, Q.; Zhang, Y.; Wang, Y.; Zhao, L.; Yu, B. *Adv. Funct. Mater.* **2007**, *17*, 2766.
(3) White, B.; Yin, M.; Hall, A.; Le, D.; Stolbov, S.; Rahman, T.; Turro, N.; O'Brien, S. *Nano Lett.* **2006**, *6*, 2095.
(4) (a) Xu, H.; Wang, W.; Zhu, W. *J. Phys. Chem. B* **2006**, *110*, 13829. (b) Yu, H.; Yu, J.; Liu, S.; Mann, S. *Chem. Mater.* **2007**, *19*, 4327.
(5) Hara, M.; Kondo, T.; Komoda, M.; Ikeda, S.; Shinohara, K.; Tanaka, A.; Kondo, J. N.; Domen, K. *Chem. Commun.* **1998**, 357.
(6) Tang, B.-X.; Wang, F.; Li, J.-H.; Xie, Y.-X.; Zhang, M.-B. *J. Org. Chem.* **2007**, *72*, 6294.
(7) Ng, C. H. B.; Fan, W. Y. *J. Phys. Chem. B* **2006**, *110*, 20801.
(8) Kuo, C.-H.; Chen, C.-H.; Huang, M. H. *Adv. Funct. Mater.* **2007**, *17*, 3773.
(9) Gou, L.; Murphy, C. J. *Nano Lett.* **2003**, *3*, 231.
(10) Siegfried, M. J.; Choi, K.-S. *J. Am. Chem. Soc.* **2006**, *128*, 10356.
(11) Siegfried, M. J.; Choi, K.-S. *Adv. Mater.* **2004**, *16*, 1743.
(12) Li, H.; Liu, R.; Zhao, R.; Zheng, Y.; Chen, W.; Xu, Z. *Cryst. Growth Des.* **2006**, *6*, 2795.
(13) Lu, C.; Qi, L.; Yang, J.; Wang, X.; Zhang, D.; Xie, J.; Ma, J. *Adv. Mater.* **2005**, *17*, 2562.
(14) Teo, J. J.; Chang, Y.; Zeng, H. C. *Langmuir* **2006**, *22*, 7369.
(15) Chang, Y.; Teo, J. J.; Zeng, H. C. *Langmuir* **2005**, *21*, 1074.
(16) Wang, Z.; Chen, X.; Liu, J.; Mo, M.; Yang, L.; Qian, Y. *Solid State Commun.* **2004**, *130*, 585.
(17) Xu, H.; Wang, W. *Angew. Chem., Int. Ed.* **2007**, *46*, 1489.
(18) Singh, D. P.; Neti, N. R.; Sinha, A. S. K.; Srivastava, O. N. *J. Phys. Chem. C* **2007**, *111*, 1638.
(19) Wang, W.; Wang, G.; Wang, X.; Zhan, Y.; Liu, Y.; Zheng, C. *Adv. Mater.* **2002**, *14*, 67.
(20) Tan, Y.; Xue, X.; Peng, Q.; Zhao, H.; Wang, T.; Li, Y. *Nano Lett.* **2007**, *7*, 3723.
(21) Jiao, S.; Xu, L.; Jiang, K.; Xu, D. *Adv. Mater.* **2006**, *18*, 1174.
(22) Caruso, F.; Caruso, R. A.; Mohwald, H. *Chem. Mater.* **1999**, *11*, 3309.
(23) Wang, L.; Sasaki, T.; Ebina, Y.; Kurashima, K.; Watanabe, M. *Chem. Mater.* **2002**, *14*, 4827.
(24) Yang, H. G.; Zeng, H. C. *Angew. Chem., Int. Ed.* **2004**, *43*, 5930.

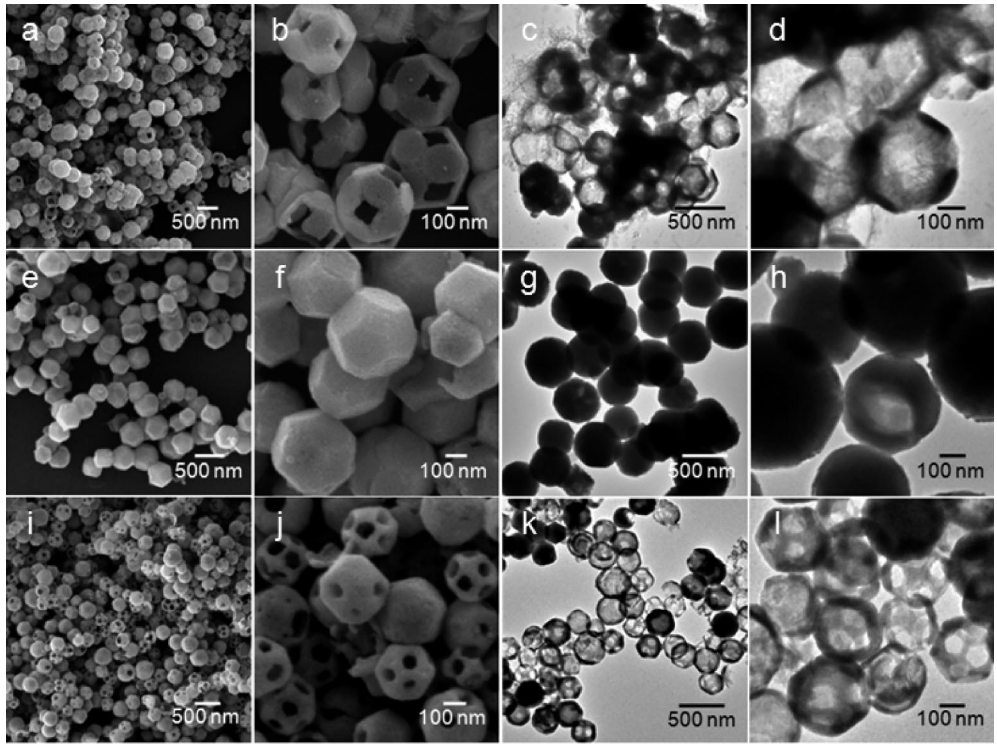

Figure 1. SEM and TEM images of the truncated rhombic dodecahedral Cu_2O nanoparticles: (a−d) type-I nanoframes, (e−h) nanocages, and (i−l) type-II nanoframes. The magnified images clearly show the hollow structures of the nanoparticles.

Scheme 1. Schematic Illustration of the Procedure for Synthesis of the Cu_2O Nanocages and Nanoframes

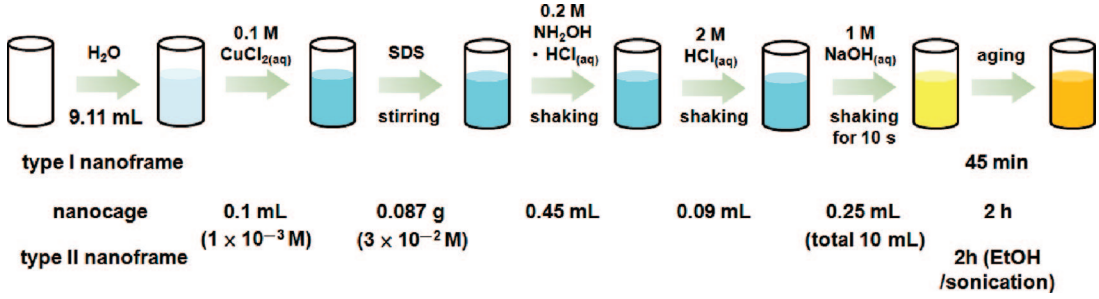

In this study, we have successfully developed a facile procedure for the synthesis of truncated rhombic dodecahedral Cu_2O nanocages and nanoframes that involves the preparation of an aqueous solution containing $CuCl_2$, sodium dodecyl sulfate (SDS) as a surfactant, hydroxylamine as a reductant, HCl, and NaOH. The nanoframes and nanocages grow by seed-particle aggregation, self-construction, and selective crystal-face etching at room temperature. Thus, this crystal growth approach is simple, low-cost, and environmentally friendly. At the present time, only one report on hollow structures having a similar morphology is known. Yang et al.[25] synthesized rhombododecahedral Ag microcages by reduction of the Ag_3PO_4 rhombododecahedral crystals formed in a mixed water/formamide solvent. These Ag microcages were polycrystals composed of Ag particles with sizes of a few hundred nanometers. We have followed the growth sequence and observed the initial generation of one type of Cu_2O nanoframes (designated as type I), which evolve into nanocages via the gradual formation of the previously empty {100} faces. Addition of ethanol leads to acidic etching of the {110} crystal faces on the nanocages, yielding nanoframes of another type (type II). We have also discovered that these nanocages can readily encapsulate various gold nanocrystals, such as nanorods and octahedra, forming interesting composite materials that may find use in various applications.

(25) Yang, J.; Qi, L.; Lu, C.; Ma, J.; Cheng, H. *Angew. Chem., Int. Ed.* **2005**, *44*, 598.

Experimental Section

Anhydrous copper(II) chloride ($CuCl_2$, 97%), hydroxylamine hydrochloride ($NH_2OH\cdot HCl$, 99%), hydrogen chloride (HCl, 37%), and SDS (99%) were purchased from Aldrich. Sodium hydroxide (NaOH, 98.2%) was purchased from Mallinckrodt. All of the chemicals were used without further purification. In a glass sample bottle, 9.11 mL of deionized water, 0.1 mL of 0.1 M $CuCl_2$, and 0.087 g of SDS (3×10^{-2} M final concentration) were mixed with vigorous stirring. After the complete dissolution of the SDS powder, 0.45 mL of 0.2 M $NH_2OH\cdot HCl$ and 0.09 mL of 2 M HCl were added with slight shaking by hand. Next, 0.25 mL of 1 M NaOH was quickly injected into the solution (generally in 1 s), and the solution was slightly shaken for 10 s, after which the colorless solution started to turn yellowish. Aging of the solution at room temperature (~20 °C) led to the formation of Cu_2O nanocages. A schematic illustration of the synthetic procedure is shown in Scheme 1. Type-I nanoframes and the nanocages were obtained after aging

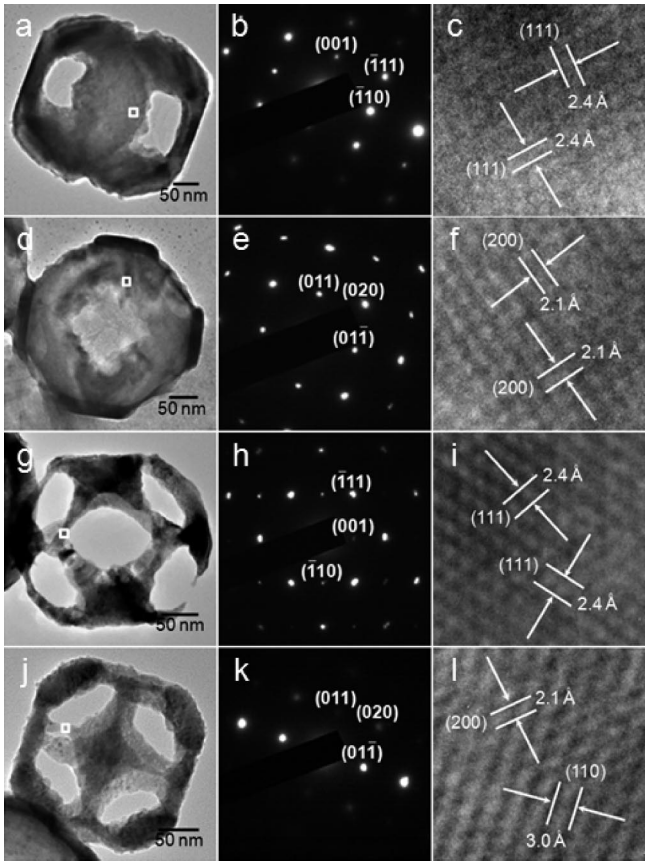

Figure 2. TEM characterization of (a−f) type-I and (g−l) type-II nanoframes viewed along different orientations. The corresponding SAED patterns recorded along the (b, h) [$\bar{1}\bar{1}0$] and (e, k) [$\bar{1}00$] zone axes indicate that the nanocages are single-crystalline and that the type-I and type-II truncated rhombic dodecahedra are constructed of {110} and {100} faces, respectively. The corresponding HRTEM images over the square regions clearly reveal the lattice fringes of the {111}, {100}, and {110} crystal faces.

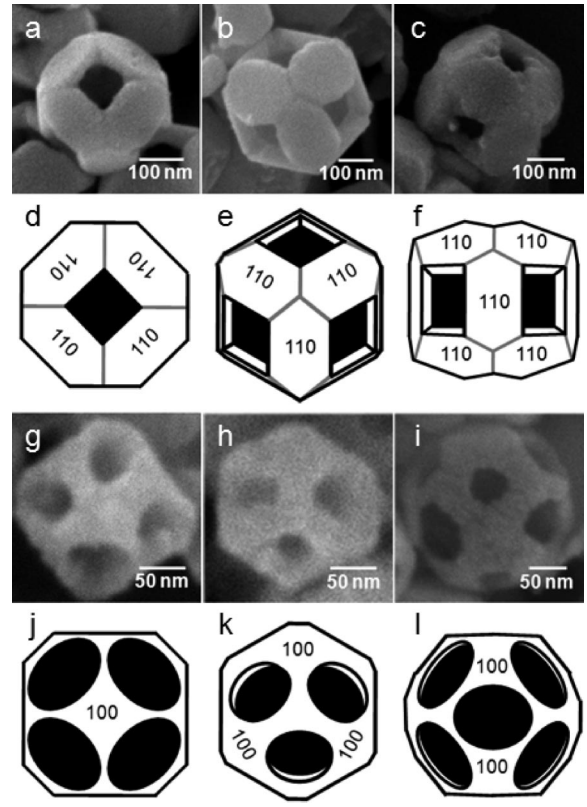

Figure 3. SEM images of single (a−c) type-I and (g−i) type-II nanoframes viewed along the (a, g) <100>, (b, h) <111>, and (c, i) <110> directions. (d−f, j−l) Schematic models corresponding to the SEM images, shown in order to illustrate their respective structures.

for 45 min and 2 h, respectively. To make type-II nanoframes, 3 mL of ethanol (95%) was added into the solution after it had aged for 2 h, and the mixture was sonicated for 1 min. The clear yellowish solution became cloudy, presumably as a result of the suspension of SDS molecules. The composites containing Au nanoparticles encapsulated in Cu_2O nanocages were prepared simply by adding Au nanocrystals (e.g., quasi-spherical particles, octahedra, and nanorods) synthesized in our laboratory into the nanocage synthesis solution before the NaOH injection step. To purify and collect these Cu_2O nanostructures, all of the solutions were washed with water and centrifuged four times at 2000 rpm for 3 min to remove the surfactant, and then the precipitate was dispersed in 1 mL of ethanol. Transmission electron microscopy (TEM) images of the products were obtained using a JEOL JEM-2100 transmission electron microscope operating at 200 kV. Scanning electron microscopy (SEM) characterization was performed on a JEOL JSM-7000F scanning electron microscope. UV−vis absorption spectra were taken using a JASCO V-570 spectrophotometer. Powder X-ray diffraction (XRD) patterns were collected using a Shimadzu XRD-6000 diffractometer with Cu Kα radiation (λ = 1.5418 Å).

Results and Discussion

After the reagents were mixed in the order specified, $Cu(OH)_2$ was initially formed from the reaction of $CuCl_2$ and NaOH and then reacted with NH_2OH to produce Cu_2O. Allowing the Cu_2O nanostructures to grow by aging the reaction mixture for ~45 min and 2 h generated type-I nanoframes and nanocages, respectively. After the formation of the nanocages, addition of ethanol followed by sonication of the solution transformed the nanocages into type-II nanoframes. Xia et al.[26] previously reported the synthesis of Au/Ag alloy nanocages and nanoframes, and these structural terms have been adopted here. Figure 1 displays SEM and TEM images of the Cu_2O nanoframes and nanocages synthesized. Type-I nanoframes (Figure 1a−d) have a peculiar morphology and clearly display square, hollow portions. These nanoframes are 300−350 nm in diameter. A close inspection of these nanostructures identified their truncated rhombic dodecahedral morphology (see Figure S1 in the Supporting Information). Each truncated rhombic dodecahedral particle contains twelve hexagonal {110} faces and six {100} faces. Thus, the type-I nanoframes are constructed of hexagonal {110} skeletons. Additional structural characterization details for these particles is provided later. Nanocages with the same truncated rhombic dodecahedral morphology (Figure 1e−h) were obtained after aging the synthesis solution for 2 h. All of the faces appeared to have been formed. TEM images revealed their hollow interiors. The nanocages have larger diameters (350−400 nm) and thicker walls than the type-I nanoframes. Type-II nanoframes are shown in Figure 1i−l. Their appearance, which includes elliptical hollow regions, is clearly different from that of type-I nanoframes, but these particles still possess the same truncated rhombic dodecahedral morphology. They have smaller diameters (200−250 nm) than the type-I nanoframes.

To further determine their structures, an extensive TEM analysis was performed. Figure 2 presents TEM images of the

(26) Lu, X.; Au, L.; McLellan, J.; Li, Z.-Y.; Marquez, M.; Xia, Y. *Nano Lett.* **2007**, *7*, 1764.

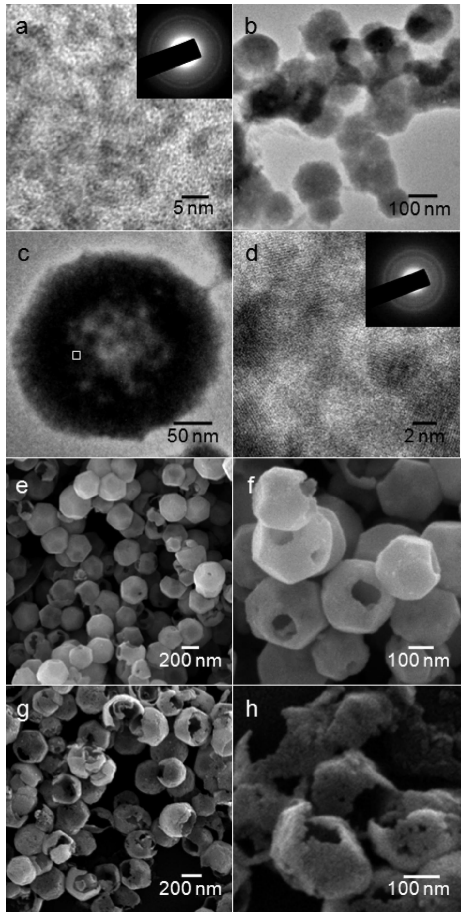

Figure 4. (a) TEM image of the small Cu_2O nanoparticles (<5 nm) formed after aging the solution for 1 min. The inset shows the corresponding SAED pattern, which is consistent with that of cubic Cu_2O. (b, c) Low- and high-magnification TEM images of the intermediate crystals (150−250 nm) captured after aging the solution for 10 min. (d) HRTEM image of the square region in (c), which reveals that these intermediate crystals are formed through the aggregation of many small Cu_2O nanoparticles. The inset displays the SAED pattern of the intermediate crystal shown in (c). (e, f) Randomly etched nanocages obtained after aging the solution for 3 h without adding ethanol. (g, h) As the aging time was extended to 6 h, most of the nanocages were broken and became collapsed pieces.

two types of Cu_2O nanoframes, their selected-area electron diffraction (SAED) patterns, and high-resolution TEM (HRTEM) images. TEM images of type-I nanoframes (Figure 2a,d) oriented on their hexagonal and square faces were obtained. Their corresponding SAED patterns recorded along the $[\bar{1}\bar{1}0]$ and $[\bar{1}00]$ zone axes verified that the hexagonal faces are the {110} crystal faces and the square, hollow regions are the unformed {100} crystal faces. Type-II nanoframes with elliptical holes have a surface structure complementary to that of the type-I nanoframes (Figure 2g,j). The corresponding SAED patterns of the type-II nanoframes recorded along the $[\bar{1}\bar{1}0]$ and $[\bar{1}00]$ zone axes confirmed that the elliptical hollow holes are produced by etching of the {110} crystal faces and that the framework is constructed of the {100} crystal faces. The HRTEM images of these two types of Cu_2O nanoframes (Figure 2c,f,i,l) exhibit clear lattice fringes with *d* spacings of 2.1, 2.4, and 3.0 Å, corresponding to the (200), (111), and (110) planes of Cu_2O, respectively; these are consistent with the results obtained from the SAED patterns. Figure 3 shows SEM images of these two types of nanoframes viewed along the <100>, <111> and <110> directions. Schematic models are also provided in order to clearly illustrate their morphologies and surface crystal faces. Their complementary structures can be recognized easily. The UV−vis absorption spectra (Figure S2 in the Supporting Information) of the Cu_2O nanocages and nanoframes showed bands that were broadened by both overlap of the band-gap absorptions and light-scattering effects.[8] The broad bands are centered at 653, 589, and 516 nm for the nanocages, type-I nanoframes, and type-II nanoframes, respectively.

The products formed at various stages of the growth process were also examined. Ultrasmall Cu_2O nanoparticles with diameters of less than 5 nm were observed after aging the reaction mixture for 1 min (Figure 4a). Much larger intermediate nanoparticles with diameters of 150−250 nm were formed after aging the solution for 10 min (Figure 4b,c). HRTEM and SAED characterization of one of these intermediate structures with a quasi-square hollow center revealed that it was composed of an aggregation and fusion of small Cu_2O nanoparticles having diameters of a few nanometers (Figure 4d). The formation of type-II nanoframes produced by a drastic etching process was also examined. Interestingly, we found that broken nanocages would form instead of type-II nanoframes if we aged the nanocage solution for an additional 1 h (i.e., a total aging time of 3 h) without adding ethanol (Figure 4e,f). Since type-II nanoframes exclusively contain the etched {110} crystal faces, we consider these faces to be more prone to etching in the formation of the broken nanocages. Addition of ethanol followed by sonication may disturb the adsorbed SDS molecules; their temporary desorption from the crystal surface may then lead to more effective etching of the {110} faces by HCl. Acidic etching of copper oxalate particles has also been described.[27] After the solution was aged for 6 h, many of the broken nanocages became collapsed pieces (Figure 4g,h). The etching process continued, and all of the Cu_2O nanocrystals disappeared after aging the solution for 12 h, as evidenced by the clear, colorless final solution.

On the basis of the above observations, the growth and etching processes of these unique Cu_2O nanostructures are presented in Scheme 2. Also, SEM images corresponding to these processes are given in Figure S3 in the Supporting Information. As soon as NaOH is added to the reaction mixture, $Cu(OH)_2$ forms instantly. Reaction of $Cu(OH)_2$ with NH_2OH produces many Cu_2O seed particles having diameters of a few nanometers. These nanoparticles quickly aggregate in order to reduce the overall energy of the system and form hollow polycrystalline intermediate structures within 10 min of reaction. The hollow intermediate structures then undergo surface reconstruction during the next 30−40 min to generate type-I nanoframes without the {100} crystal faces. This rapid crystal growth continues, with Cu_2O seed particles adsorbing onto the nanoframes and filling the {100} faces. Truncated rhombic dodecahedral Cu_2O nanocages with diameters larger than those of the type-I nanoframes are gradually synthesized during the next ~75 min of reaction. It appears that within the first 2 h of reaction, the crystal growth process dominates the etching process. When ethanol is added and sonication of the solution is applied, the adsorption of SDS molecules on the nanocage surfaces likely is temporarily disrupted, and the solution becomes cloudy for several minutes. SDS may serve the role of protecting the Cu_2O nanocrystals from direct etching by HCl; removal of SDS facilitates the reaction of Cu_2O and HCl to form $HCuCl_2$. The faster etching rate on the {110} faces than on the {100} faces transforms the nanocages into type-II

(27) Zhao, X.; Yu, J. *J. Cryst. Growth* **2007**, *306*, 366.

Scheme 2. Schematic Illustration of the Growth and Etching Mechanisms in the Synthesis of the Nanoframes and Nanocages

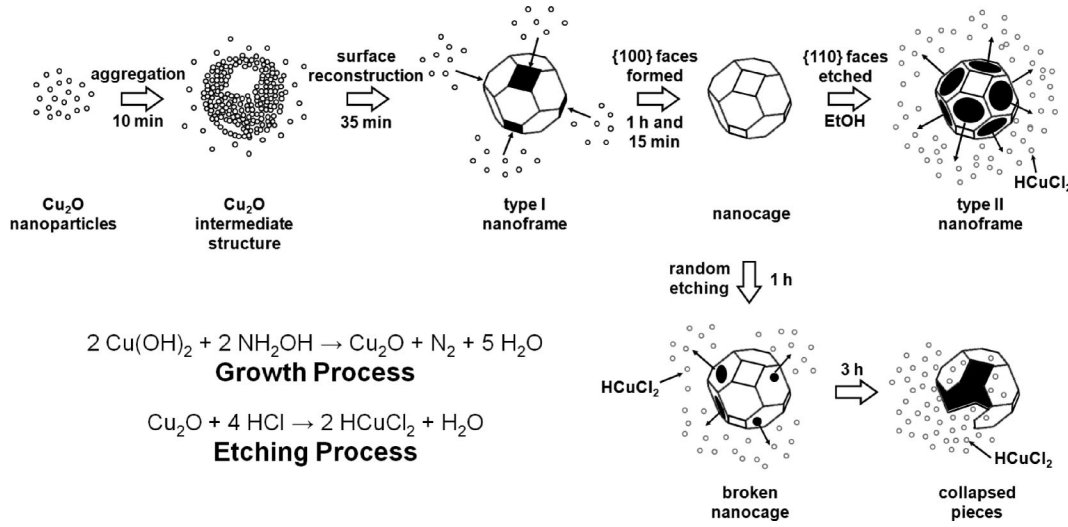

$$2\,Cu(OH)_2 + 2\,NH_2OH \rightarrow Cu_2O + N_2 + 5\,H_2O$$

Growth Process

$$Cu_2O + 4\,HCl \rightarrow 2\,HCuCl_2 + H_2O$$

Etching Process

nanoframes with thinner walls and smaller particle sizes. The thinner walls also cause a substantial loss of peak intensities in their XRD patterns (Figure S4 in the Supporting Information). When the 2 M HCl solution was not introduced, solid cuboctahedral Cu_2O nanocrystals rather than nanocages and nanoframes were prepared. The solution pH dropped from 11.68 in the absence of the HCl solution to 5.54 after its addition (measured at an aging time of 2 h). Without the addition of ethanol, acidic etching of the nanocages still occurs but proceeds at a lower rate. Incomplete coverage of SDS molecules on the crystal surfaces makes the nanocages susceptible to attack by HCl and leads to broken nanocages and finally collapsed pieces 4 h after the nanocage formation.

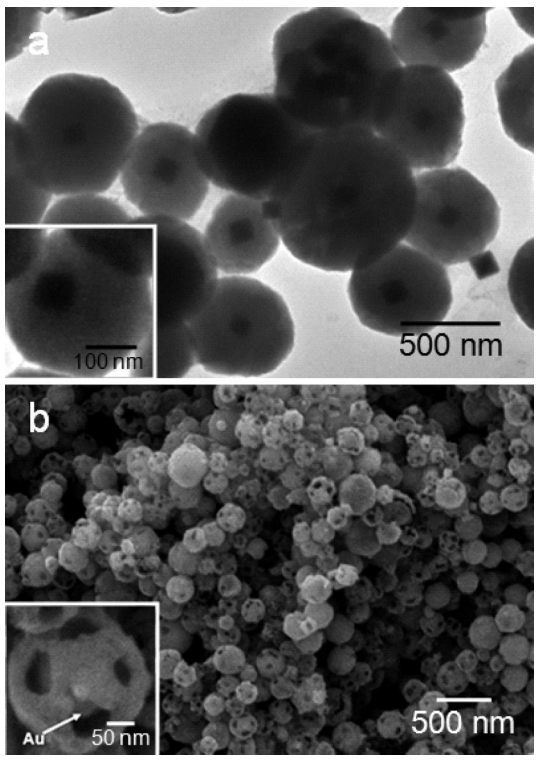

Figure 5. (a) TEM image displaying octahedral gold nanocrystals encapsulated inside the truncated rhombic dodecahedral Cu_2O nanocages. The TEM image in the inset shows that the gold octahedron is not centrally located inside the cage. (b) SEM image of type-II nanoframes with encapuslated gold octahedra. The nanoframes are noticeably smaller than the nanocages as a result of acidic etching. The inset shows a gold octahedron trapped inside the nanoframe.

In order to test whether the nanocages with empty interiors could be used to encapsulate nanocrystals, octahedral gold nanocrystals with sizes ranging from several tens of nanometers to ~100 nm were added to the reaction mixture, and the solution was aged for 2 h. Figure 5a shows TEM images of the resulting truncated rhombic dodecahedral Cu_2O nanocages with encapsulated gold octahedra. Interestingly, practically every nanocage contains only a single gold nanoparticle. Although the octahedral gold nanocrystals may appear to be located in the center of the nanocages, SEM images of some partially broken nanocages (Figure S5b in the Supporting Information) revealed that the gold octahedra may actually be anchored to the interior side walls of the nanocages (also see the inset of Figure 5a). In this respect, this core−cage nanocomposite structure is different from the more typical Au@metal oxide core−shell structures, in which the oxide shells completely cover the encapsulated gold cores and there is no empty space between them.[28−30] Figure 5b displays SEM images of type-II nanoframes with encapsulated gold octahedra that formed after addition of ethanol to the nanocages and sonication of the solution. Because the pores of the nanoframes are smaller than the enclosed octahedral gold nanocrystals, the gold octahedra cannot escape from the nanoframes. Essentially no gold octahedra can be found outside the nanoframes. Quasi-spherical gold nanoparticles with sizes of tens of nanometers have also been found to attach to the interior side walls of the nanocages (data not shown). Similarly, only one gold nanoparticle is confined within each nanocage.

High-aspect-ratio gold nanorods with lengths longer than the nanocage diameter were also used to see if encapsulation would still occur.[31,32] Figure 6 shows the TEM images of the resulting nanocomposite products formed after aging the reaction mixture for 2 h. Surprisingly, the nanocages adopt a capsular shape to accommodate the long nanorods, and each elongated nanocage

(28) Wang, Y. Q.; Nikitin, K.; McComb, D. W. *Chem. Phys. Lett.* **2008**, *456*, 202.
(29) Lu, Y.; Yin, Y.; Li, Z.-Y.; Xia, Y. *Nano Lett.* **2002**, *2*, 785.
(30) Liz-Marzán, L. M.; Giersig, M.; Mulvaney, P. *Langmuir* **1996**, *12*, 4329.
(31) Wu, H.-Y.; Chu, H.-C.; Kuo, T.-J.; Kuo, C.-L.; Huang, M. H. *Chem. Mater.* **2005**, *17*, 6447.

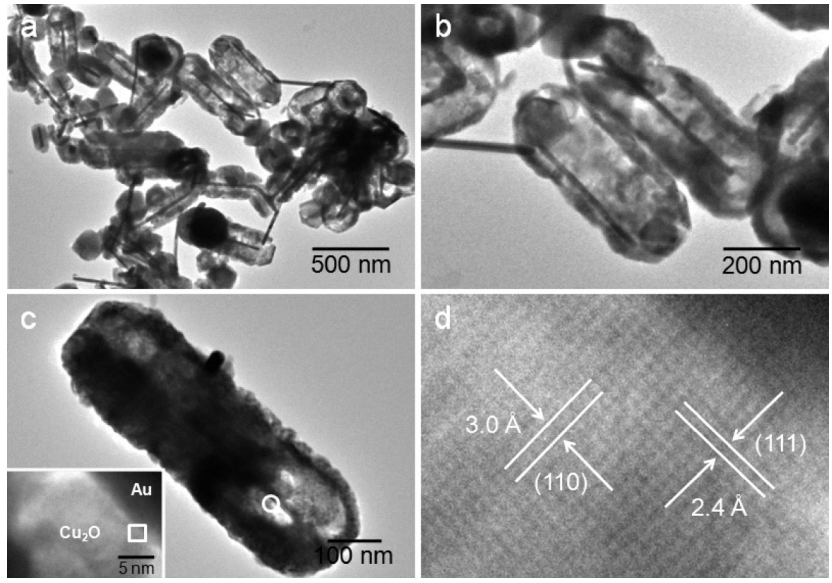

Figure 6. (a) TEM image of gold nanorods encapsulated inside Cu_2O nanocages having a capsular shape. (b) Enlarged view of a region in (a), showing that the gold nanorod is not necessarily located in the middle of the cage. Hexagonal gold nanoplates may also be included inside the nanocages. (c) TEM image of a single nanorod−nanocage composite structure. The inset shows the magnified image of the circled region. A Cu_2O crystal grows over the surface of this part of the nanorod. (d) HRTEM image of the square region in the inset of (c). At the interfacial region of the gold nanorod and the Cu_2O crystal, clear (111) and (110) lattice fringes of Cu_2O can be observed, with the (111) lattice planes growing parallel to the long axis of the nanorod.

holds just one nanorod inside. It is noticeable that the gold nanorods usually reside centrally inside the nanocages, but sometimes they can be found near the interior side walls of the cages (see Figure S5d,e in the Supporting Information for SEM images and Figure 6b for a TEM image). From the contours of the nanocages shown in Figure 6a, it seems that at least some of the elongated nanocages still attempt to maintain the truncated rhombic dodecahedral structure, suggesting that closely spaced Cu_2O nanocage intermediate products can be connected during their growth with the assistance of the nanorod support. Individual capsular nanocages were examined to see how such nanocomposite structures can be formed (see Figure 6c and Figure S5c in the Supporting Information for TEM images). An interfacial region between the gold nanorod and a Cu_2O crystal growing over the surface of the nanorod was studied. The Cu_2O crystal was attached to the gold nanorod over a length of ~15 nm. Figure 6d is the HRTEM image of the interfacial growth region. Clear (111) and (110) lattice fringes can be observed, with the (111) lattice planes running parallel to the long axis of the nanorod. The crystal can serve as a bridge to link the nanorod to the nanocage. It is possible that many more Cu_2O seed particles could continuously adsorb onto these bridging crystals and gradually form a capsule-shaped cage. Formation of elongated nanocages with nanorods residing near the inner walls is similar to the condition for the formation of the octahedron-encapsulating truncated rhombic dodecahedral nanocages, and this nanocage growth process is also favorable.

Conclusions

In conclusion, we have developed a simple procedure for the preparation of Cu_2O nanocages and nanoframes and confirmed their unusual truncated rhombic dodecahedral structure. Type-I nanoframes containing just the {110} skeleton faces were the first to form after mixing the reagents. Further crystal growth transformed the nanoframes into nanocages with the formation of the {100} faces. Acidic etching by HCl via the addition of ethanol to the nanocage solution, which disrupts the adsorption of the surface-capped SDS molecules and facilitates preferential etching of the {110} faces, resulted in the formation of type-II nanoframes. The nanocages can encapsulate various gold nanostructures, such as octahedra and nanorods. The process of formation of these encapsulated species was investigated. These core−cage composite materials may find use in various applications, such as drug delivery, molecular sensing, and so on. Other metal and semiconductor nanostructures may also be encapsulated using these Cu_2O nanocages in order to provide enhanced properties and functions.

Acknowledgment. We thank the National Science Council of Taiwan (Grant NSC95-2113-M-007-031-MY3) for support of this research.

Supporting Information Available: Illustration of the geometry of a truncated rhombic dodecahedron, SEM images of the crystal growth and etching processes, UV−vis absorption spectra and XRD patterns of the nanoframes and nanocages, and SEM and TEM images of the core−cage composite structures. This material is available free of charge via the Internet at http://pubs.acs.org.

JA804625S

(32) Wu, H.-Y.; Huang, W.-L.; Huang, M. H. *Cryst. Growth Des.* **2007**, *7*, 831.